

INITIAL RESULTS FROM EUROPEAN ROAD SAFETY INSPECTION (EURSI) MOBILE MAPPING PROJECT

Conor Mc Elhinney, Pankaj Kumar, Conor Cahalane and Timothy McCarthy

National Centre for Geocomputation (NCG),
National University of Ireland Maynooth (NUIM),
Maynooth, Co. Kildare, Ireland
conormce@cs.nuim.ie, tim.mccarthy@nuim.ie
<http://www.eursi.com/>

KEY WORDS: LIDAR, point cloud, road edge extraction, mobile mapping, unsupervised segmentation

ABSTRACT:

Mobile mapping systems are becoming a popular method for collecting high quality near 3D information of terrestrial scenes. Modern mobile mapping systems can produce millions of georeferenced points per minute. These can be used to gather quantitative information about surfaces and objects. With this geospatial data it is becoming possible to segment and extract the road surface. In this paper, we will detail a novel LIDAR based road edge extraction algorithm which is applicable to both urban and rural road sections.

1 INTRODUCTION

Road transportation in Europe is a high value sector having a turn-over of almost €2.5 trillion in 2006 with almost 293 million vehicles travelling over 5 million kilometres of road-network (EU energy and transport in figures, 2008). In the same year, just under 43,000 people were killed on European roads (EU energy and transport in figures, 2008). In 2001, the European Commission drafted an objective to reduce the present number of deaths by half to below 25,000 by 2010 (New Solutions to reduce the number of fatalities on European roads, 2008). There are three main areas that influence road-safety; vehicle, driver behaviour and route environment or infrastructure. Safety aspects of road vehicle are covered by a number of eSafetyAware initiatives such as the European new car assessment (EuroNCAP) programme. Improvements in driver behaviour are covered by a number of initiatives including training, driver licensing, enforcement as well as ongoing research projects. Road infrastructure safety has become a key area of interest within the transportation sector and is supported by a number of directives and initiatives. A Tunnel Directive came into force 1 May 2004, promoting greater driver safety in tunnel environments. A road infrastructure safety management directive (Directive 2008/96/EC) has already been adopted by the Commission and is currently passing through various legislative processes. This directive focuses on four specific areas; road-safety impact assessment, road-safety audit, high accident concentration ranking and safety inspections of existing roads. This directive will come into force December 2010 and member states will have to adopt "guidelines in order to support the competent entities". These entities include both public and private organisations involved in implementing the directive.

Over 40% of European road related fatalities and injuries occur along rural or secondary road networks (Gatti et al., 2007). Rural roads constitute a large percentage of the total route network throughout Europe (EU energy and transport in figures, 2008). Road safety audits and inspections vary across Europe for example, only 10 out of 20 European countries surveyed were obliged to carry out Road Safety Audits in 2007 (Falco et al., 2007). The current road infrastructure directive seeks to address this shortcoming by compelling member states to adopt and implement more standardised road safety assessment procedures. Current road inspection surveys are manually intensive and involve an engineer annotating a digital map or using spatially referenced

video to manually classify various features along the route (Gatti et al., 2007, EEnink et al., 2007, Dutch national road safety research institute, 2007, Lynam et al., 2005, Falco et al., 2007). A recent research call highlighted the requirement for common evaluation tools and implementation strategies in carrying out these inspections and assessing risk along route corridors (ERANET, 2009).

The chief objectives of the "European Road Safety Inspection" EuRSI mobile mapping research tasks are to investigate various automated and semi-automated approaches to processing geocoded LiDAR and image data in order to extract features and reconstruct the route corridor in 3D. The first stage of a 3D route corridor reconstruction is segmentation of the data, specifically road segmentation. Information about the road and its surface is becoming increasingly important for the fields of road safety and road maintenance amongst others. To obtain accurate information about the road and its surface, we first need to extract the edges from the LIDAR and subsequently the road points between these edges. We have developed an algorithm to extract the left and right road edges applicable to all types of roads.

Segmenting roads is required in fields such as mapping, autonomous vehicle navigation and road safety. The segmentation of roads using LIDAR is a relatively new field of research with the first reported results from vehicle based systems in 2001 (Manandhar and Shibasaki, 2001). Road segmentation using LIDAR data recorded from aerial systems has been the most prevalent (Toth and Grejner-Brzezinska, 2006, Elberink and Vosselman, 2009, Mumtaz and Mooney, 2009). However, the field of vehicle based LIDAR is becoming more common leading to novel road segmentation algorithms being developed for these systems (Rongben et al., 2005, Kodagoda et al., 2006, Takagi et al., 2006, Yu and Zhang, 2006, Jaakkola et al., 2008, Yuan et al., 2008, Jihyun and Crane, 2009). The largest portion of the road segmentation algorithms have focused on urban roads which are highly structured (Toth and Grejner-Brzezinska, 2006, Elberink and Vosselman, 2009, Mumtaz and Mooney, 2009, Manandhar and Shibasaki, 2001, Rongben et al., 2005, Kodagoda et al., 2006, Takagi et al., 2006, Toth and Grejner-Brzezinska, 2006, Yu and Zhang, 2006, Jaakkola et al., 2008, Yuan et al., 2008). Some of the road segmentation approaches developed are based on fitting lines to the LIDAR data to search for a horizontal straight line (Yuan et al., 2008), using a precomputed DTM to select the relevant LIDAR

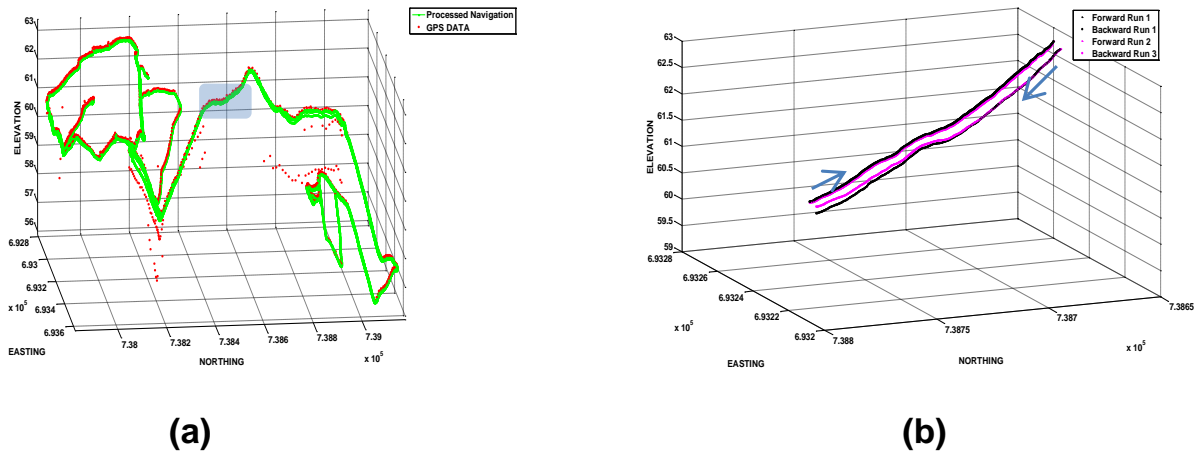


Figure 1: Navigation example: Processed navigation data plotted along with GPS data with highlighted section(a), navigation data from highlighted section from the same section of road from two passes, twice up and twice down the road.



Figure 2: LIDAR from typical secondary roads: (a) an urban road and (b) a rural road.

points (Elberink and Vosselman, 2009) and curb detection (Toth and Grejner-Brzezinska, 2006, Yu and Zhang, 2006, Jaakkola et al., 2008). A more general solution has been developed by Jihyun et al. (Jihyun and Crane, 2009). They calculate the slope of cross section of lidar data and use this to determine the road edge. There is also a large field of road following algorithms using LIDAR data designed for use on autonomous vehicles (Rasmussen, 2006, Morales et al., 2009). The majority of these algorithms do not attempt to find the edges, border or the surface of the road but aim to determine accurately where the road is and more importantly for the vehicle where it isn't.

2 MOBILE MAPPING SYSTEM

Mobile platforms which combine mapping and navigation sensors on a rigid mount to collect geospatial data are called mobile mapping systems. A mobile mapping system (MMS) can directly georeference the onboard mapping sensors relative to the navigation sensor. These MMSs can be generally classified into three categories: space borne, airborne or terrestrial systems. The main differences between these systems is the resolution, scale, accuracy and completeness of the output geospatial data. In this paper we are focusing on terrestrial based MMSs. These produce point clouds with the highest density of points per m^2 .

The first terrestrial based MMS was developed in the 1980s by the Ohio State University for highway inventories (Novak, 1993). This system combined GPS technology alongside stereo vision and colour cameras. MMSs are now being produced commercially (Kremer and Hunter, 2007, Haala et al., 2008) with high density point clouds and an accuracy of better than 30mm. We

True heading [deg]	0.01
Roll/Pitch [deg]	0.005
Position X and Y [m]	0.02
Position Z [m]	0.05
Measurement Rate	100Hz

Table 1: IXSEA LANDINS specifications

have just completed design and construction of a novel mobile mapping experimental platform (XP-1) which we will now discuss.

2.1 XP-1

Our MMS comprises of an IXSEA LandINS GPS/INS, a 3D LIDAR sensor, and imaging system. At the heart of the LandINS INS is a high-grade, solid-state fibre optic gyroscope (FOG) technology with a drift rate of better than 0.05/hr as detailed in Table 1. A distance measurement instrument (DMI), fitted to the wheel of the vehicle, captures movement over ground and is used in computing final navigation solution during post-processing. The specifications for the Riegl VQ-250 LiDAR are shown in Table 2. The LIDAR system is mounted on the back of the van at a 45° angle from both the horizontal and vertical axis of the vehicle. This produces scan lines which are not orthogonal to the road and produces richer 3D information. It captures up to 1 million points every 3.5 seconds using a 300kHz sensor. Typical data capture for VQ-250 LiDAR system is 20Gb per hour.

There are six progressive scan cameras (1280*1024) that can be placed anywhere on top of the roof-rack or inside the windscreen of survey vehicle. A FLIR thermal (un-cooled) SC-660 camera as

Measurement Rate	300kHz
Minimum Range [m]	1.5
Accuracy [m]	0.01
Precision [m]	0.01
Intensity	16 bit
Field of View [deg]	360
Scan Speed	100Hz

Table 2: Riegl VQ-250 specifications

well as an innovative 5-CCD multispectral camera enables visible, infrared and thermal spectral signatures along route corridors to be investigated. Active infrared LED illumination enables the mobile mapping system to operate in the dark or low-light conditions. Total image data throughput is in the order of 250Mb/s. A power sub-system onboard the vehicle is capable of supplying upto 3kW of power. Synchronisation and triggering of all sensors is centrally controlled over LAN using a high speed GPS timing device. Three 4U 19" servers provide data logging services and are fitted with removable disks to facilitate fast data processing. An operator sits beside the driver and controls all on-board systems using a central data acquisition console. System initialisation usually takes 20 minutes before the vehicle can begin surveying. Most of this time is spent ensuring that coarse and fine alignment of navigation system is carried out correctly.

A qualitative examination of the navigation data output from the IXSEA LANDINS was carried out by driving an approximately 5km test section of road. The navigation sensor was in operation continuously for an hour and eleven minutes. We drove up the test section of road and back twice over the course of this time. The results after the two stage processing of the navigation data is shown in Fig. 1. In Fig. 1(a) the result of the first processing stage of the GPS is displayed with red circles. The green line is the final navigation obtained after the second stage which is processing the GPS and the INS together. In this figure, it can be seen that the second stage of processing corrects for some of the errors in the GPS. We have highlighted a section in blue and displayed this in Fig. 1(b). In this section of the road we have driven the same area times, twice up and twice back. The strong correlation between the forward and backward runs demonstrates the accuracy of the navigation data. Two examples of the georeferenced LIDAR point clouds from secondary roads are shown in Fig. 2. A typical urban secondary road is displayed in Fig. 2(a) with a structured road boundary in the form of curbs on both sides of the road along with a potential error source of parked cars. In Fig. 2(b) we display a typical rural road with an uneven non-uniform road boundary. In the next section we will describe our automatic algorithm which can extract the road edges from both these roads.

3 ALGORITHM

We have developed a two stage algorithm for extracting the road edge from the LIDAR and navigation data, the workflow of which is shown in Fig. 3. The first stage of this algorithm creates a set of road cross sections. In the second stage we process these cross sections into 2D lines. These lines are then analysed based on the slope, returned intensity, returned pulse width and proximity to the vehicle to determine the road edges.

The first stage of our algorithm takes as input the LIDAR point cloud and navigation data. This stage of the algorithm is explained in Fig. 4. We first take every tenth GPS time from the navigation and store them in z . $L_t(x, y)$ is the set of lines of length l which are orthogonal to the road. These are computed by creating a line orthogonal to the vehicles direction of travel

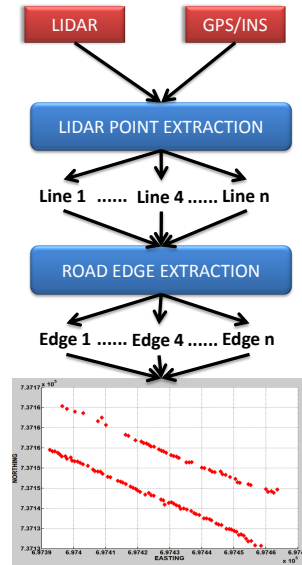


Figure 3: Road edge extraction algorithm workflow.

using the (easting, northing, heading) attribute of the navigation. All LIDAR points whose (easting, northing) position is within a distance of μ from the line are then stored in $Line_t(x, y, z)$ along with the attributes of amplitude and pulse width.

The set of $Line_t(x, y, z)$'s are then input into stage two of the algorithm which is displayed in Fig. 5. The first step is to remove points whose elevation is too high and fit a 2D cubic spline to the data. We assume that the vehicle is on the road and with our knowledge that the LIDAR is approximately 2.4m above the road surface we remove all points which are greater than the $GPS(elevation) - 2$. We then take the northing and elevation values from $Line_t(x, y, z)$ (the (y, z) values) and fit a 2D cubic spline (Luhmann et al., 2006) storing it in $North_t(y, z)$. The slope of the spline is calculated $Slope_t(y, z)$ and all the peaks and troughs in the slope above a normalised threshold are found and stored in $P(y, z)$. The base of these peaks and troughs $B(y, z)$ are potential edges of the road. By filtering $B(y, z)$ based on an LIDAR intensity and pulse width threshold we remove non-edge candidates. The closest left and right $B(y, z)$ is taken as the left and right edge of the road. We then find the closest original (x, y, z) LIDAR point to these edges and store it in $Edge_t(x, y, z)$. An example of the resulting edges is shown in Fig. 6. From this figure it can be seen that the left edge of the road is of higher quality than the right edge, this is due to the XP-1 system containing one LIDAR and driving on the left side of the road. This could be overcome by adding a second LIDAR to the vehicle or driving the road section a second time from the opposite direction.

4 EXPERIMENTS

We demonstrate the effectiveness of our algorithm using two road sections, an urban and secondary road section. The algorithm parameters were constant for both experiments, a line length $l = 14m$, and two line widths of $\mu = 0.1m$ and $\mu = 0.3m$, the amplitude threshold was set to 2700 and the pulse width threshold was set to 30. The vehicle was travelling at approximately 30km/h in both cases.

In our first road section, the road is a regional urban road as shown in Fig. 7(a). The edge on both sides of the road is a curb. The results from our algorithm for the plan view, view from the drivers perspective for $l = 0.1m$ are shown in Fig. 7(a-b) and for $l = 0.3m$ are shown in Fig. 7(d-e), respectively. An interesting area

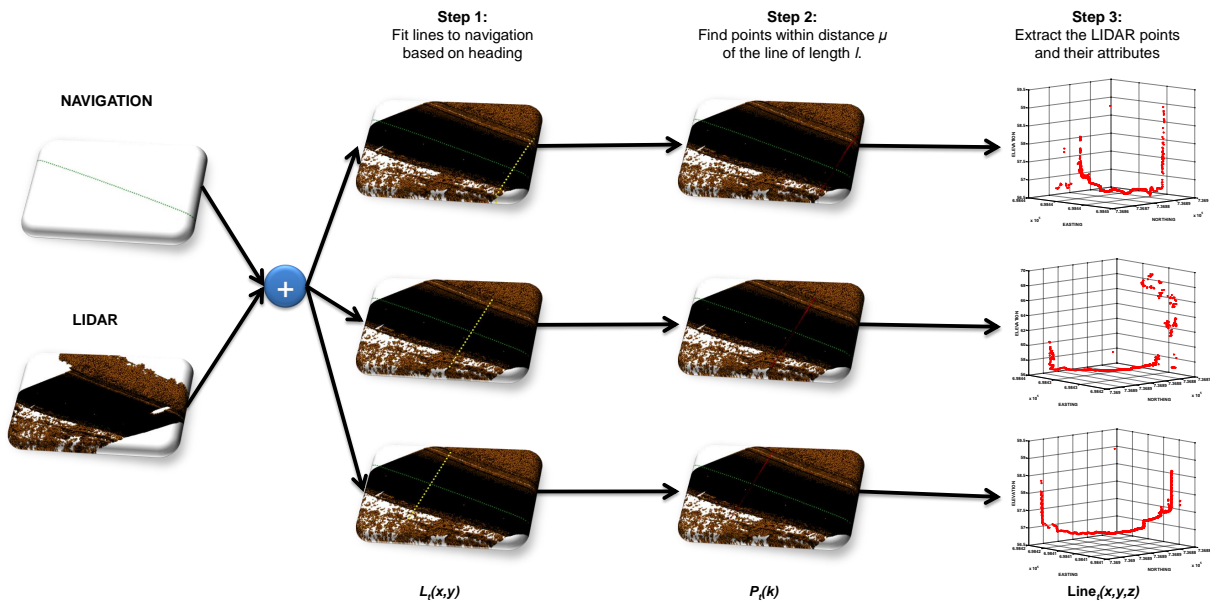


Figure 4: LIDAR point extraction, Stage 1 of our road edge segmentation algorithm.

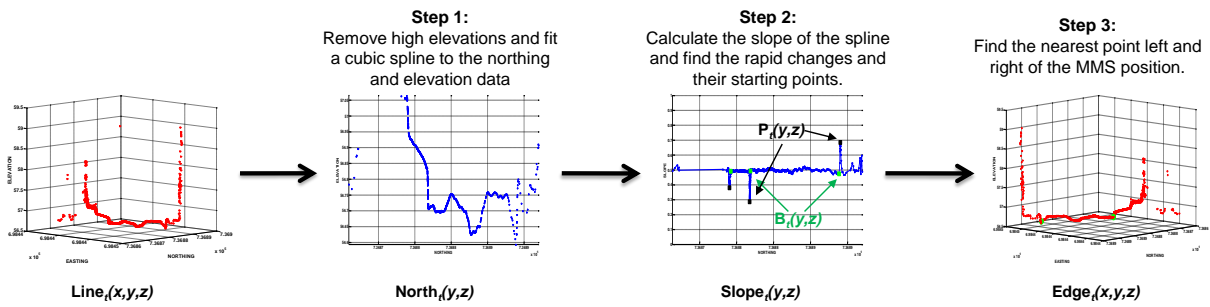


Figure 5: Road edge extraction, Stage 2 of our algorithm.

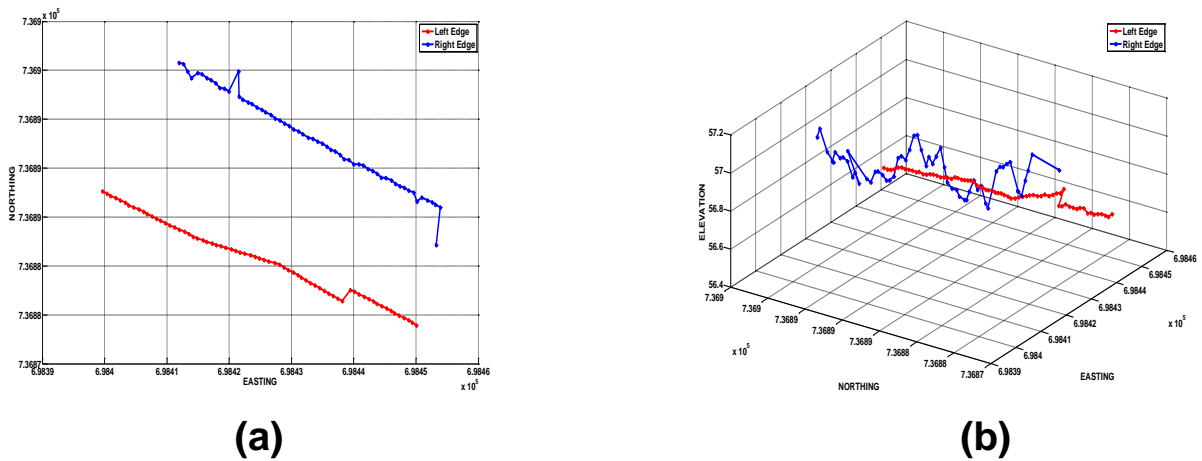


Figure 6: Plot of road edges output from our algorithm: (a) Plan view and (b) plot in 3D.

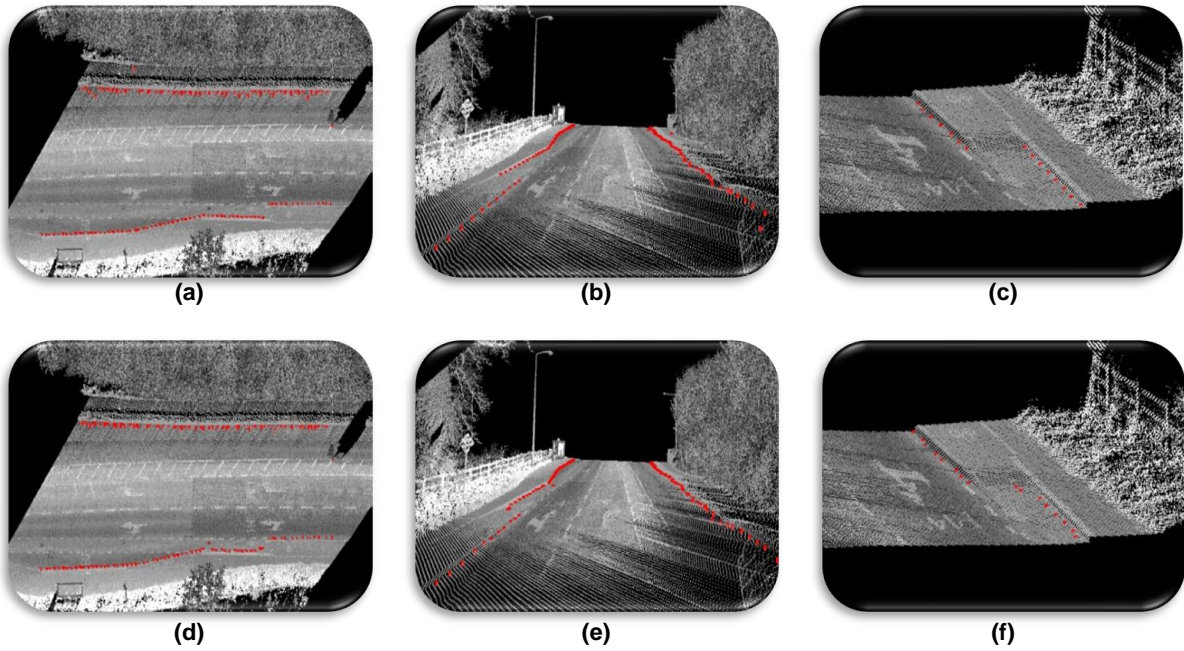


Figure 7: Road edge segmentation on regional roads with curbs with estimated road edges highlighted in red applied with a 0.1m line width (a) plan view of road, (b) view along road, (c) zoomed in view of bike path becoming road and applied with a 0.3m line width (d) plan view of road, (e) view along road and (f) zoomed in view of bike path becoming road.

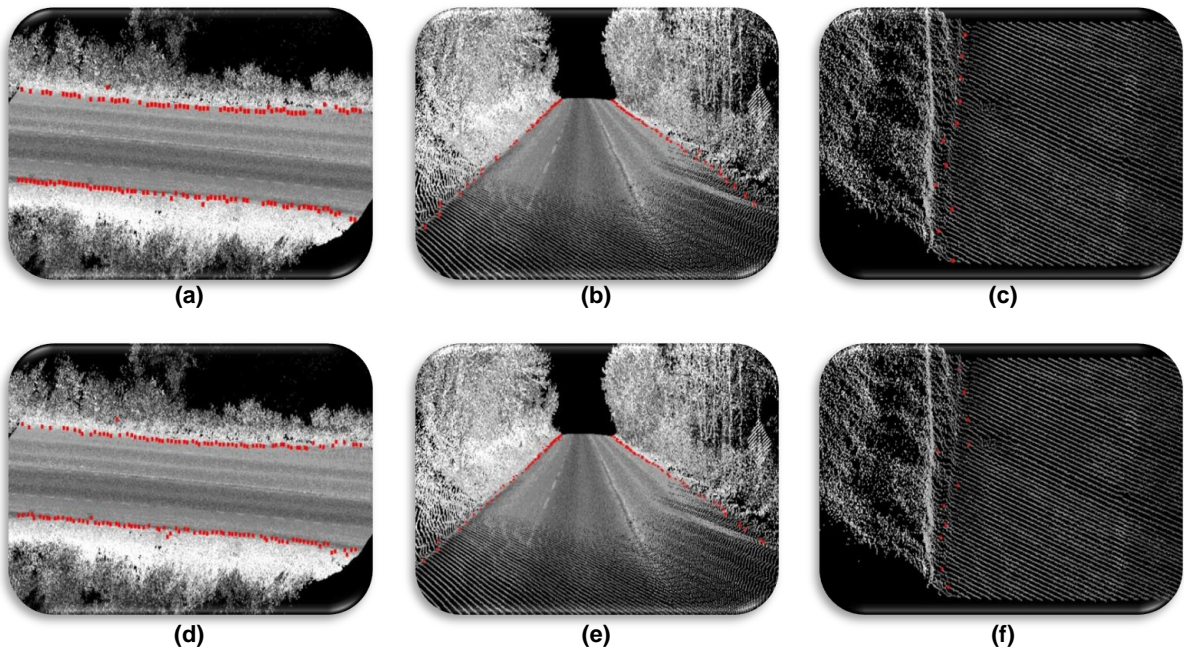


Figure 8: Road edge segmentation on regional roads with varied road edges with estimated road edges highlighted in red applied with a 0.1m line width (a) plan view of road, (b) view along road, (c) zoomed in road edge and applied with a 0.3m line width (d) plan view of road, (e) view along road and (f) zoomed in road edge.

in this road is a bike path which is on the footpath and joins the road due to an oncoming bus stop, which moves the left road edge nearly 1.5m. Our algorithm successfully detects this change as shown in Fig. 7(c,f).

The second road section is from a rural secondary road where the road edges are not easily defined. They range from cracks in the road to declinations and elevations. The road section is shown in Fig. 8(a). The results from our algorithm for the plan view, view from the drivers perspective for $l = 0.1m$ are shown in Fig. 8(a-b) and for $l = 0.3m$ are shown in Fig. 8(d-e), respectively. An area of the left road edge is shown in Fig. 8(c,f). In this small 2m area the road edge could not be described easily. However, our algorithm is able to successfully find the road edge. In both of the road sections there are areas where both the $l = 0.1m$ and the $l = 0.3m$ results outperform each other. We intend to optimise the systems parameters through more exhaustive testing.

5 CONCLUSION

The field of mobile mapping and road segmentation have been discussed in this paper. We have detailed a novel method for automatically extracting the road edge from secondary roads. This algorithm works on both urban and rural road sections. Using LIDAR point clouds collected from our XP-1 MMS we have verified our algorithm and presented the results. Determining the accuracy of the approach is not a trivial task as it would involve manually selecting the road edge, we are currently investigating the best approach to test the accuracy of our algorithm. A number of areas require further work, one area is that our algorithm does not use the easting value of the LIDAR point cloud to calculate the road edge. We believe the results would be improved on by using this attribute. Due to our use of an individual laser scanner there is a lower density of points on the right edge of the road than the left edge resulting in less accurate right edge extraction. A double pass approach where we drive the road twice once in each direction, processing each run would increase the accuracy of the right edge extraction.

ACKNOWLEDGEMENTS

Research presented in this paper was funded by the ERA-NET SR01 projects and a Strategic Research Cluster grant (07/SRC/I1168) by Science Foundation Ireland under the National Development Plan. The authors gratefully acknowledge this support.

REFERENCES

Dutch national road safety research institute, 2007. The Road Safety Audit and Road Safety Inspection. SWOV Fact Sheet.

EENink, R., Reurings, M., Elvik, R., Cardoso, J., Wichert, S. and Stefan, C., 2007. Road Safety Impact Assessment and Accident Prediction Model - Tools, Recommendation and Implementation Aspects.

Elberink, S. J. O. and Vosselman, G., 2009. 3D information extraction from laser point clouds covering complex road junctions. The Photogrammetric Record 24(125), pp. 23–36.

EU energy and transport in figures, 2008.

Falco, F., Proctor, S. and Gonzalez, E., 2007. The European road safety auditor training syllabus.

Gatti, G., Polidor, C., Galvez, I., Mallschütze K., Jorna, R., Leur, M. V. D., Dietze, M., Ebersbach, D., Lippold, C., Schlag, B., Weller, G., Wyczynski, A., Iman, F. and Aydin, C., 2007. Safety Handbook for Secondary Roads.

Haala, N., Peter, M., Kremer, J., Hunter, G., Stuttgart, U. and Cloud, P., 2008. Mobile lidar mapping for 3d point cloud collection in urban areas a performance test. In: ISPRS Congress, ISPRS, Beijing, China, pp. 1119–1124.

Jaakkola, A., Hyyppä, J., Hyyppä, H. and Kukko, A., 2008. Retrieval Algorithms for Road Surface Modelling Using Laser-Based Mobile Mapping. Sensors 8(9), pp. 5238–5249.

Jihyun, Y. and Crane, C., 2009. Evaluation of terrain using LADAR data in urban environment for autonomous vehicles and its application in the DARPA urban challenge. In: ICCAS-SICE, 2009, IEEE, Fukuoka, Japan, pp. 641 – 646.

Kodagoda, K., Wijesoma, W. and Balasuriya, A., 2006. CuTE: curb tracking and estimation. IEEE Transactions on Control Systems Technology 14(5), pp. 951–957.

Kremer, J. and Hunter, G., 2007. Performance of the StreetMapper Mobile LIDAR Mapping System in "Real World" Projects. In: Photogrammetric Week, Vol. 07pp, Stuttgart, Germany, pp. 215–225.

Luhmann, T., Robson, S., Kyle, S. and Harley, I., 2006. Close Range Photogrammetry Principles, Methods and Applications. Whittles, Scotland.

Lynam, D., Sutch, T. and Trl, J. B., 2005. European road assessment programme pilot phase technical report.

Manandhar, D. and Shibasaki, R., 2001. Vehicle-borne laser mapping system (VLMS) for 3-D GIS. In: IEEE Geoscience and Remote Sensing Symposium, Vol. 00, IEEE, Sydney, Australia, pp. 2073–2075.

Morales, Y., Tsubouchi, T. and Yuta, S., 2009. Vehicle 3D localization in mountainous woodland environments. In: IEEE Intelligent Robots and Systems, IEEE, St. Louis, USA, pp. 3588–3594.

Mumtaz, S. A. and Mooney, K., 2009. A semi-automatic approach to object extraction from a combination of image and laser data. In: ISPRS, Vol. XXXVIII, ISPRS, Paris, France, pp. 53–58.

New Solutions to reduce the number of fatalities on European roads, 2008.

Novak, K., 1993. Mobile mapping systems: new tools for the fast collection of GIS information. In: B. P. C. Whitmill, A. Douglas, B. L. Foley, B. Huberty and L. D. (eds), Proceedings of SPIE, Vol. 188, SPIE, Orlando, USA, pp. 188–198.

Rasmussen, C., 2006. A hybrid vision+ lidar rural road follower. In: IEEE Robotics and Automation, Vol. pp, IEEE, Orlando, USA, pp. 156–161.

Rong-ben, W., Bai-yuan, G., Li-sheng, J., Tian-hong, Y. and Lie, G., 2005. Study on curb detection method based on 3D range image by LaserRadar. In: IEEE Intelligent Vehicles Symposium, IEEE, pp. 845–848.

Takagi, K., Morikawa, K., Ogawa, T. and Saburi, M., 2006. Road environment recognition using on-vehicle LIDAR. In: IEEE Intelligent Vehicles Symposium, IEEE, Tokyo, Japan, p. 120125.

Toth, C. and Grejner-Brzezinska, D., 2006. Extracting dynamic spatial data from airborne imaging sensors to support traffic flow estimation. ISPRS Journal of Photogrammetry and Remote Sensing 61(3-4), pp. 137148.

Yu, C. and Zhang, D., 2006. Road Curbs Detection Based on Laser Radar. In: IEEE Signal Processing, IEEE, Beijing, China, pp. 8–11.

Yuan, X., Zhao, C.-x., Cai, Y.-f., Zhang, H. and Chen, D.-b., 2008. Road-surface abstraction using lidar sensing. In: IEEE Control, Automation, Robotics and Vision, IEEE, Hanoi, Vietnam, pp. 1097–1102.